



## MICRO STRIP FED CIRCULAR SHAPPED 4-ELEMENT MULTIBAND MIMO ANTENNA FOR 5G WLAN APPLICATIONS

<sup>1</sup>B Santhikiran, <sup>2</sup>Nikhil Lam, <sup>3</sup>V Eswar Kumar, <sup>4</sup>Imran MD

<sup>1</sup>Associate Professor, <sup>2,3,4</sup>Student,

<sup>1,2,3,4</sup>Dept. of Electronics and communication Engineering,

<sup>1,2,3,4</sup>Andhra Loyola Institute of Engineering and Technology, Vijayawada, A.P, India.

**Abstract:** This work presents innovative design of Multi Input and Multi Output system for coming generation with 5G, 6G and beyond mobile terminals to the proposed system is composed, is confident of a main design that is Circular shaped antenna. To make the design cost effective FR-4 is used as a substrate, the proposed antenna is designed with a 4-Element, is Resonating at 3.4GHz attaining a less than 10db Bandwidth, The signal transformed into a MIMO array of 4-Elements with an overall dimensions of 102\*102\*1.6 mm<sup>3</sup> providing patterns diversity characteristics, isolation and ECC by radiating the elements. A number of studies such as Wi-Fi Router for human activities requires single mode and dual mode scenarios and these effects covers the principle performance of the system are present. The Envelop Correlation Coefficient (ECC) is quantity for all the scenarios and it is found that the ECC is less than 0.08, for any case. The main advantage of proposed designed over, available designs in the literature concentrating all most of all of the main Substrate is empty and providing wide space for different Sensor system, Mobile technology components. A literature comparison of the proposed system is also present to Validate the proposed model, a prototype fabricated and results are tested on the real time Wi-Fi Router. The simulated results are in an Excellent Unity with the measured results. The performance parameters of the design are calculated with the measured results.

**Index Terms -** Wi-Fi Routers, MIMO, ultra wide band, mobile terminals and smart phones.

### I. INTRODUCTION

Because of the high data rates, optical performance, delays, the price and the requirement for better channel network of communication capacity, For large-scale coverage, low 5G NR sub-6 GHz frequencies are currently being used [1, 2, 3]. As a result, the new frequency band on 5G New WLAN Radio and INSAT is optimized for a wide range of applications requiring multi-gigabit data rates per second [4, 5]. The frequency of 5G wave applications has been increased in the US (28.0 GHz, 37.0 GHz, and 39.0 GHz), Japan (27.5.0–28.8.0 GHz), China (24.25–27.50 GHz, 37.0–43.50 GHz) and Korea (28.0 GHz) [6].

Ultra Wide Band (UWB) is a wireless communication technology has become increasingly important in recent years., meets the needs of modern communication systems in both broad bandwidth and high profitability. In wireless communication, however, the deterioration of multiple paths has a significant impact on UWB technology. The usage of MIMO Antenna, which improves the power of wireless communication networks, is one answer to the blurring of many ways. For MIMO antennas, distinguishing between several antennas during the creation of an interconnected ground plane is a tough task [7-8]. Decoupling structures [9], Only a few examples have been proposed to increase antenna separation in MIMO systems: Defected Ground Structure [10], Electronic Band Gap [11-12], and Split Ring Resonator [13]. Wide bandwidth is another necessity of UWB technology. Which is impossible to reach with standard patch antennas due to their low bandwidth. Various techniques, such as a slotted micro strip-fed [14], 4 elements that include a rectangular angle and corners [15], a single pole antenna with Split Ring Resonator and the ring-shaped globe [17]. It is also advisable to have the same object among objects in the MIMO antenna, as this increases the actual use of the antennas [18].

The use of 2 MIMO antennas on a single mm-wave [19] and dual [20] frequency bands is proposed, as well as a [19] connected profile and [20] with a different ground structure. Because two dipole structures are not large enough to cater to a large number of customers, four port-operated antennas are much needed. In the mm-wave single states [21, 22], dual [23, 24], and wide-band [25,

26, 27], four port antennas are proposed, all of which are excluded [27] with a connected ground plane. The proposed antennas [23, 24] consider a dual-frequency band with access to the mm-wave application band, but does not include the entire 5G band, so the four-port MIMO is preferred. Although the proposed antennas in [25, 26, 27] surround the 5G spectrum, the dimensions of the recommended antennas in [25, 26] is greater than the suggested note. Although the proposed antenna [27] is small and covers a wide range of mm 5G wave, it has a different base, As a result, it's not ideal for real-time applications.

For wideband mm-wave applications, a small antenna with four vertical ports (24 \*24 mm<sup>2</sup>) with a slot that is elliptical in the center, a coplanar feed that has been modified, and a lower plane section. The increase in the bandwidth is obtained via adjusting with extreme caution, design the ground plane and the elliptical slot in the centre. The suggested 4-Element antenna works in range of 24.8 to 26.0 GHz and has a separation of more than 20 dB between ports. MIMO diversity and satisfied diversity are added to the integrated profile. HFSS is used to simulate and test a design. The proposed antenna creates radiation patterns in Omni directional with a gain of 5.80db,82% low efficiency, and also it gives ECC=0.08, DG=9.99db in a whole range of spectrum frequency based on the results the antenna is simulated and observed on HFSS toll and Vector Network Analyzer .the suggested work is applicable for 5G applications.

**II. GEOMETRY OF ANTENNA DESIGN**

Antenna with a monopole, folded gap and short edges is shown in Fig.1. The delivery of this monopole antennacomes from the coplanar waveguide (CPW). The following figures show the basic formulas in the design of monopole antennas for CPW feeds.

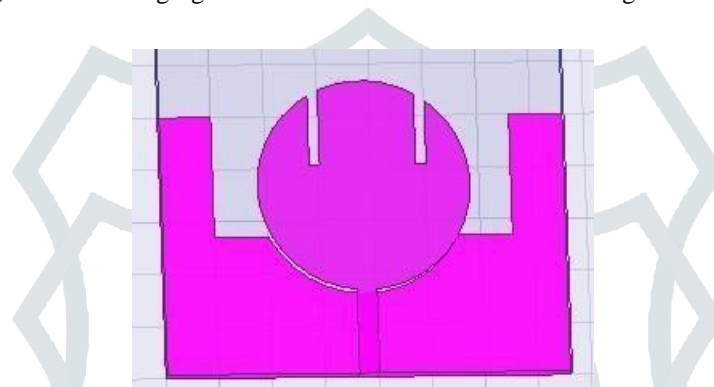


Fig.1 The Proposed Antenna in Single pole.

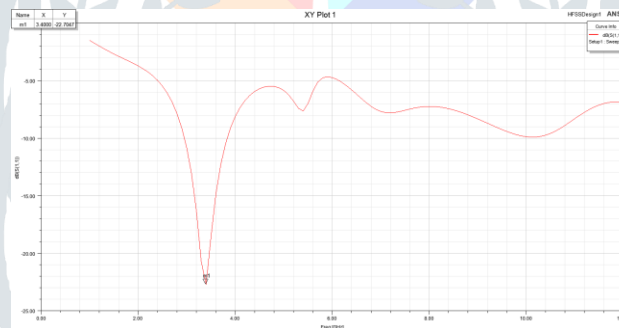


Fig.2 S11 plot of single pole antenna.

CPW is determined by the following equation:

$$E_{\text{reff}} = (Err+1)/2 \{ \tanh[0.775 \ln(h/G)+1.75] + Kg/h \times [0.004 - 0.7k + 0.01(1 - 0.1Er)(0.25+k)] \} \tag{1}$$

where,

$$k = W/W + 2G \tag{2}$$

W= Center conductor width, h = Substrate thickness,

G =There is a gap space between the conductor and the ground.

The formula for calculating the ratio of first order elliptic integral and its complement is

$$Z_{oCPW} = 20\pi / \sqrt{E_{\text{reff}}} K'(k) / K(k) \tag{3}$$

$$K'(k) / K(k) = [\pi / \ln(2(1 + \sqrt{k}) / (1 - \sqrt{k}))] \text{ If } 0 < k < 0.707$$

$$K'(k) / K(k) = [\ln(2(1 + \sqrt{k}) / (1 - \sqrt{k})) / \pi] \text{ If } 0.707 < k < 1 \tag{4}$$

From equation 4, the theoretical values are of  $E_{\text{reff}} = 2.809$ ,  $Z_{oCPW} \sim 48\Omega$  for the dimensions of  $W = 2.0\text{mm}$ ,  $h=1.60\text{mm}$ ,  $G = 0.30\text{mm}$  and  $r = 4.40\text{mm}$ . Ultra-wideband has achieved its and which ranges is 2.4GHz to 18.6GHz with bandwidth of 15.6GHz. H-slots near dual slots are equipped with a rectangular radiation features to achieve dual band notch structures. The following figures in 5.6 can be used to determine the maximum H size, the U-shaped stubs set in the frequency of the middle notch band.

$$L_s = \lambda_g / 4 \tag{5}$$

$$\lambda_g = \lambda_0 \sqrt{\epsilon_r}$$

$\lambda_g$  = guided in wavelength

$\lambda_0 = c_0 / f$  = wavelength in free space,

f

r = center frequency of notch band

$c_0$  = light of velocity

$\epsilon_r$  = dielectric constant

Figure 1 shows a statistical view on a perforated monopole radio wave and an Circular shaped monopole system that receives circular slots, This receiving wire is made a prototype on the polyimide substrate with a diameter of  $80 \times 80 \times 1.6 \text{ mm}^3$  This proposed receiving monopole antenna has a transmission capacity from, 2.2 GHz - 18.4 GHz, and 3.6 GHz (WiMAX) and 8.3 GHz (military and radar) scores, as Shown in Fig.2, In this way, the intended and repeated acquisitions should be the same. In addition, the impact of the redesigned CPW feed is evaluated using only the U-shaped slots, and the display coefficient's performance is tested. In fig.1 the Two tiny patches designed with a radius of 1.5 mm is placed besides the given patch. A Circular slot is designed to increase the performance of the given antenna and also find the amount of correlation in different space sizes. Improves 10 dB impedance bandwidth performance and display coefficient levels, especially for low frequency bands, when operating from 24.8 to 26.0GHz.

### III. 4- ELEMENT MIMO ANTENNA

After researching the single antenna element, it is arranged in an orthogonal rotation with its ground, as shown in Fig. 3. The minimum distance between MIMO elements is maintained by k in order to minimize compounding effects and ensure spatial diversity, Performance. In addition, the proposed design avoids obstructions of similar members, requiring a distance between elements of the same members in order to be cut according to the connector space.

HFSS software was used to model the MIMO four-element antenna design model. Excess current distribution at various frequencies (3.655 GHz, 5.8 GHz, 10.145 GHz, 20.145 GHz, and 30.205 GHz) is investigated by regenerating one hole while leaving the others disconnected at a load of 50 X, as Shown in Figures.5-9, It shows that the antenna excitement in various operating waves reduces leakage, which is manifested due to local variability and a different floor profile. In addition, the distribution parameters can be used to justify the current power combined at least from one pole to another, when the gap between the holes is greater than 20 dB, as seen in Fig.7.

Despite the antenna's great performance (as shown in Fig. 4), its practical application is limited due to the soil profile. However, it requires at least one common method that connects all sub-planes to be embedded in a standard printed circuit board (PCB) structure without compromising the performance of individual ports.

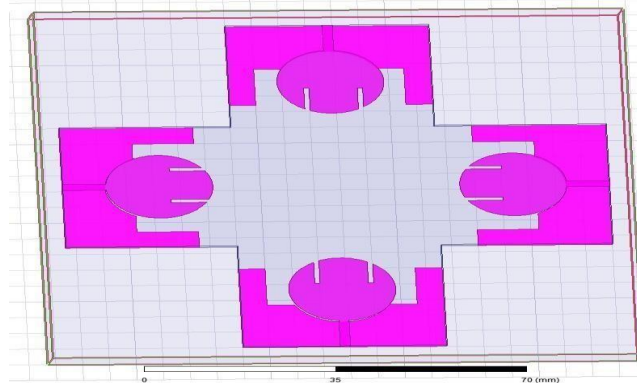


Fig.3 Proposed 4 Element Orthogonal Antenna.

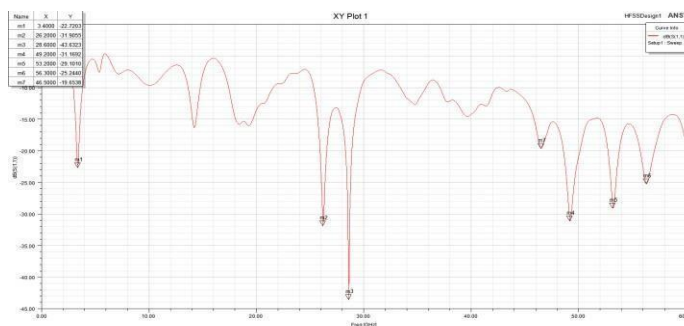


Fig.4 S11 Plot of Proposed 4 Elements Orthogonal Antenna.

The ECC values of the proposed model with an orthogonal 4 element MIMO antenna are approximately 0.08. If the ECC value of the antenna is approximately 0.09, it is not the best antenna to use; however, when the converted ECC value is less than or equal to 0.08, this model is the best. When the value of ECC is reduced, segregation also suffers. We have chosen this shape instead of f because we want the ECC value to be less than 0.08. With our proposed antenna, we can get an ECC value of approximately 0.08.

As illustrated in Figures 5–9, the mentioned current distribution was evaluated at various frequencies (3.655 GHz, 10.145 GHz, 20.145 GHz, and 30.205 GHz) to have a better understanding of the MIMO series' performance and correlation between items. The power integration in the operational bandwidth is quite low, even with the addition of an L-shaped patch that forms a connected ground structure, indicating a significant separation between objects. Researchers have been drawn to a better distinction between certain elements, and several methods have actually been introduced to do so. From Fig. 4, the planes upper and lower in our design produce an Excellent 20 dB transmission frames and width passing bandwidth (79.35 percent) 24.8 to 26.0GHz.

#### IV. DESIGN AND EVALUATION OF 4 ELEMENT ANTENNA

From the figures [11-12] proposes the fabricated antenna top and bottom views on a polyimide substrate. Figures [13- 15] illustrates the coefficient to reflect the suggested antenna test results. At frequencies between 24.8 and 26.0GHz, the predicted coefficient value is better as compared to 10 dB., and nearly identical to the measured result. Although the results are within the capabilities of 5G applications, the modest differences in performance are attributable to network connectivity and performance limitations. MIMO antenna applications for chosen frequency bands are also provided.

Shows the setting of the radiation pattern setting in the anechoic chamber with one object activated at the same time, whereas the other three elements share the same load.

**Table 1: Comparison of Proposed H-Shaped & Circular Shaped Antennas**

PARAMETES	H-Shaped	CIRCULAR
Size	80*80*1.6mm <sup>3</sup>	102*102*1.6mm <sup>3</sup>
Impedance Bandwidth	S11<-10db (5.6GHz-5.9GHz)	S11<-10db (24.8GHz- 26.0GHz)
ECC	0.09	0.08
Directivity Gain	9.96~10	9.99~10
Peak Gain	5.09	5.80
Radiation Efficiency	80%	82%
Mutual Coupling	<-20db	<-50db
Isolation	Split ring Resonator	Split ring Resonator
Feeding	CPW	Microstrip
Substrate	Polymide	FR-4

## V.MIMO DIVERSITY SCHEMES

To expand the actual implementation of the 4 element MIMO antenna performs a variance analysis according to the DG and ECC. In the MIMO 4-element flexible antenna, the operating conditions of the MIMO variant according to ECC are calculated, where values are obtained using below equation (a) [30].

### 1. SURFACE CURRENT DISTRIBUTION:

At the 3.4GHz and 5.8GHz notch, as well as the 10GHz, 20GHz and 30GHz performance band, the current overhead distribution of the four-dimensional antenna is under investigation.

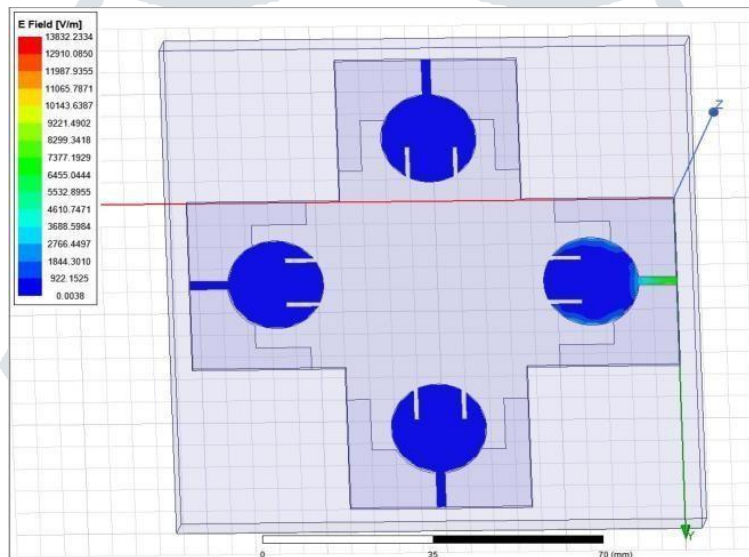


Fig.5 E-Field at 3.4GHz

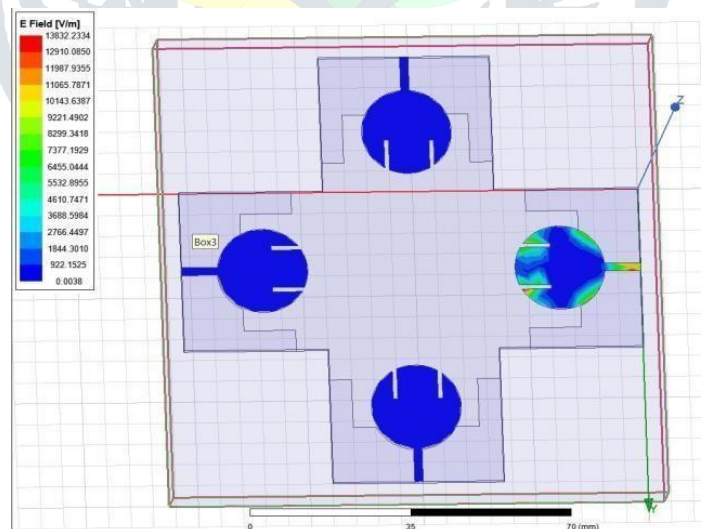


Fig.6 E-Field at 5.8GHz

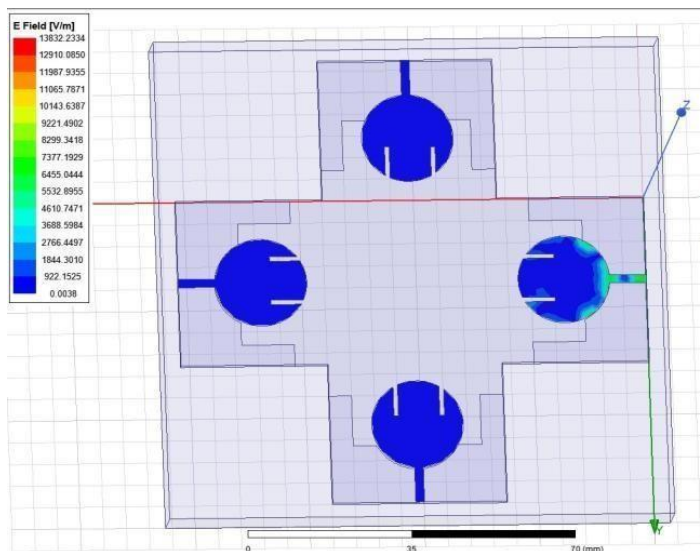


Fig.7 E-Field at 10GHz

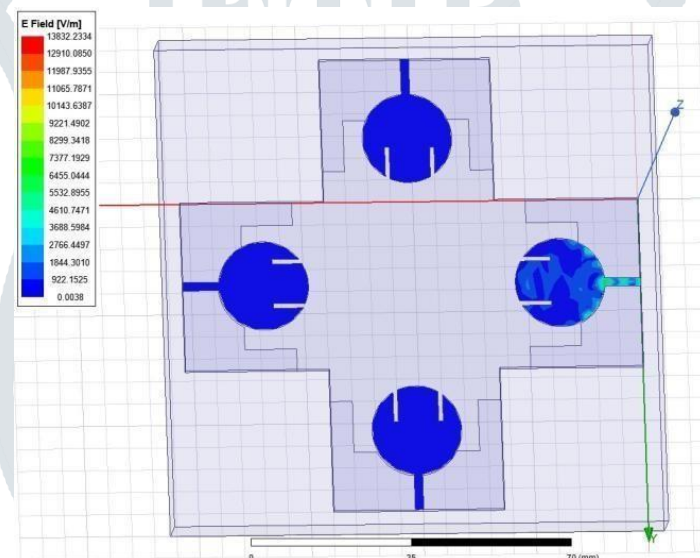


Fig.8 E-Field at 20GHz

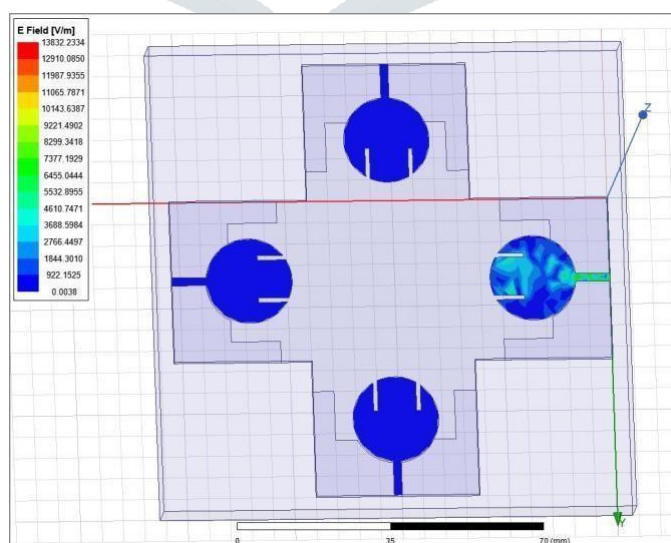


Fig.9 E-Field at 30GHz

Figures [17-22] shows two-dimensional radiation designs in the polar directions of the two parts of the MIMO radio cable at 10 GHz and 5.8 GHz frequencies on various plane, such as x, y, and z plane. The x-plane, or receiving plane, is used by two MIMO components that receive cables. Finally, co-division occurs by Gain-phi value and co-division occurs by Gain-theta value.

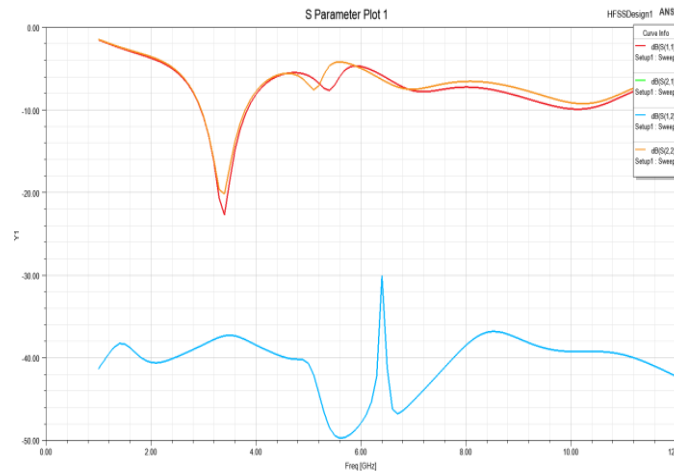


Fig.10 S parameters of 4Element Orthogonal MIMO Antenna.

2. ENVELOPE CORRELATION COEFFICIENT (ECC):

The differences between the 2 MIMO radio cable components are considered. The integrated connection of the MIMO radio port1 & port2 can produce radiant design. The envelope co-relation coefficient of any Multi input Multi output antenna should be less than 0.5 to indicate good variability. Both the measured and experimental ECC ratings are 0.02 in excess of the entire 5G range switching indices.

$$ECC = \frac{|(S11*S12) + (S21*S22)|}{(1-|S11|^2-|S21|^2) * (1-|S22|^2-|S12|^2)} \text{-----(a)}$$

3. DIVERSITY GAIN (DG):

DG is measured by the antenna parameters, which is defined as

$$DG = 10\sqrt{(1-ECC^2)} \text{-----(b)}$$

VI. FABRICATION RESULTS AND RADIATION PATTERNS

Figures [17-22] Shows the calculated gain as well as the efficiency of the designed antennas. The proposed mm- wave antenna's gain is >5dB and Efficiency is of 85 percent in the necessary band.

Based on operating parameters such as used material, port number, connected ground profile, location, bandwidth performance, profitability, efficiency, isolation, and ECC, the Suggested MIMO antenna for the Suggested wave is compared to other antennas. The proposed states are integrated and give larger bandwidth, sufficient profitability, and efficiency over the stipulated bandwidth, with strong separation from the lower ECC, based on the Table.1 comparison.

In various ways, the Suggested MIMO small Antenna small mm-wave 4 differs from pre-designed radiators:

- Focuses on the width of the sub-mm-wave frequency.
- Construction is small, measuring only 24\* 24 mm2.
- Even with a connected ground profile, there is a high degree of isolation between ports.
- Increase radiation efficiency by using a polyimide substrate.
- Easy to make because of its orderliness and simplicity.

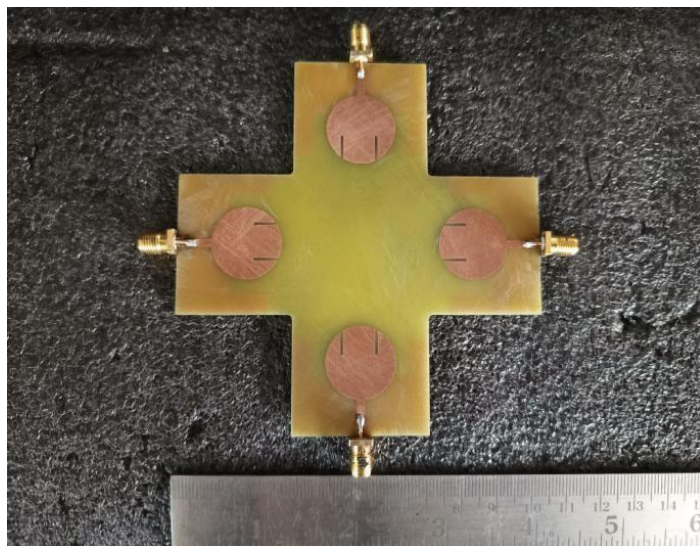


Fig.11 Fabricated Antenna's Top view

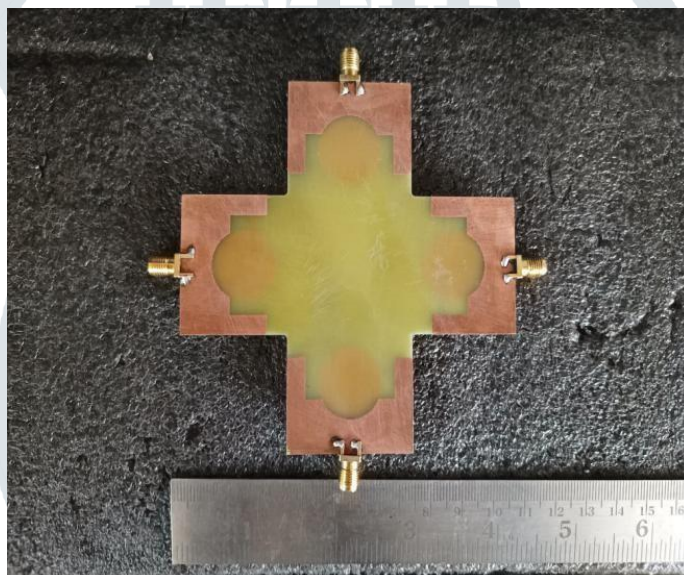


Fig.12 Fabricated Antenna's Bottom view

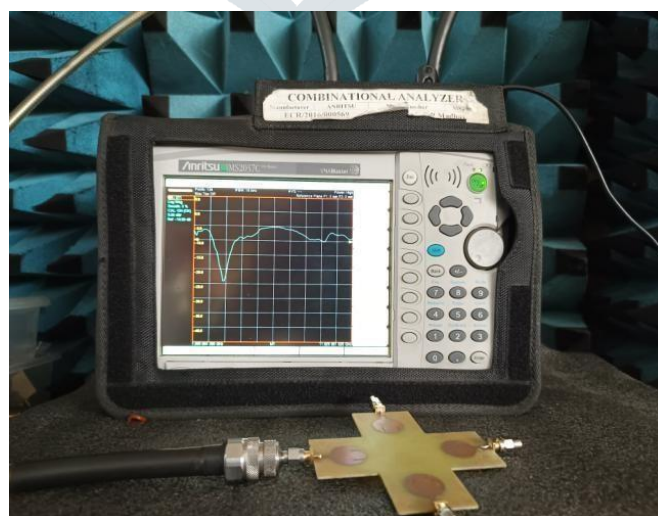


Fig.13 S11 Plot of Fabricated Antenna From VNA

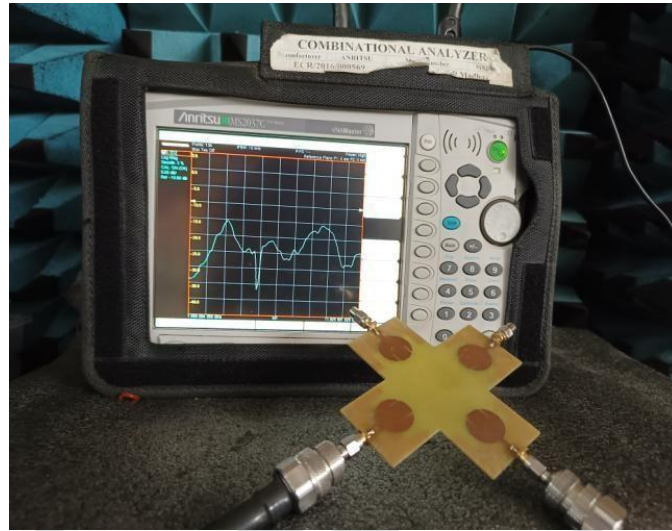


Fig.14 VNA results of S12/S21 Plot of Fabricated Antenna

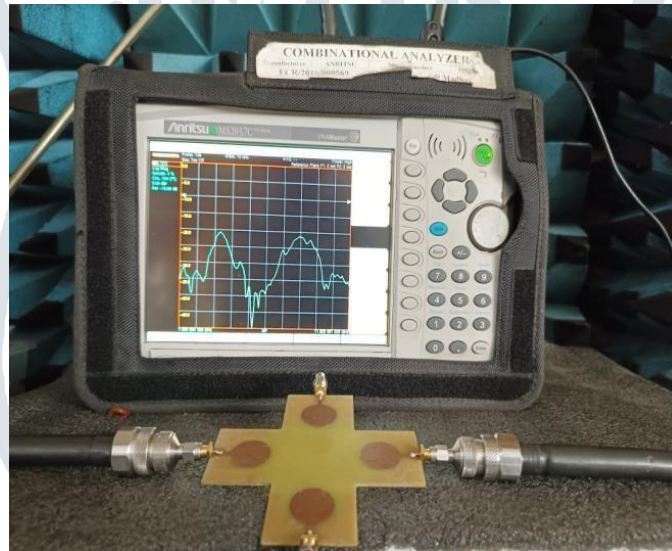


Fig.15 VNA results of S13 Plot of Fabricated Antenna

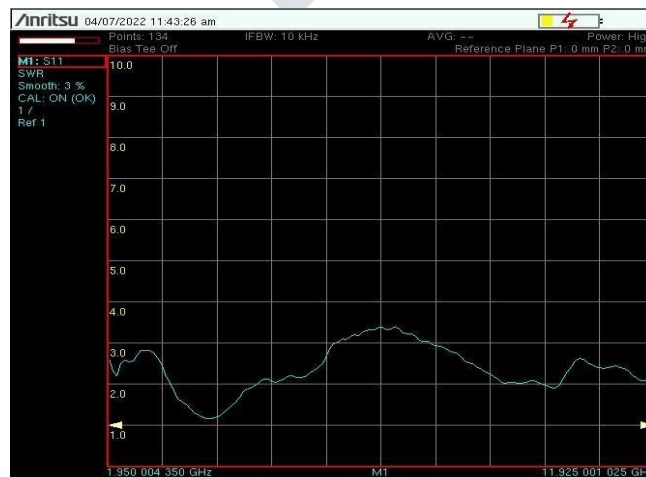


Fig.16 VNA results of VSWR Plot of Fabricated Antenna

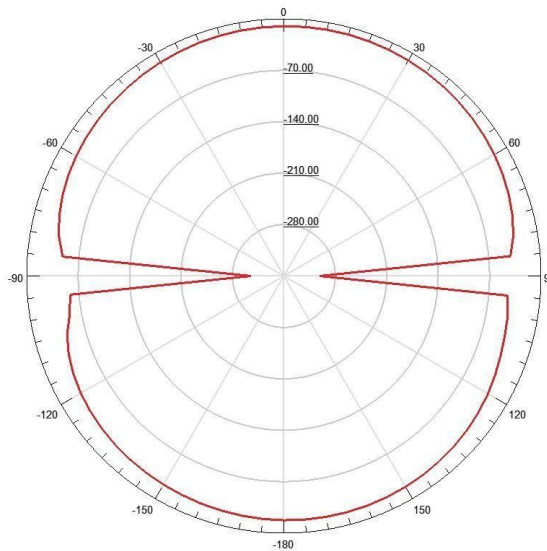


Fig.17 X plane radiation pattern at 3.4GHz

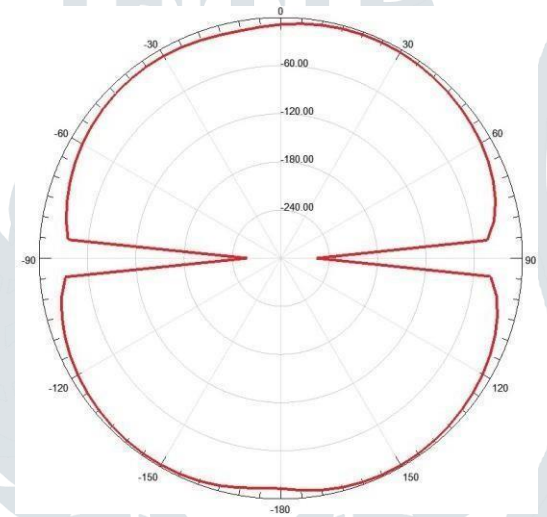


Fig.18 X plane radiation pattern at 10GHz

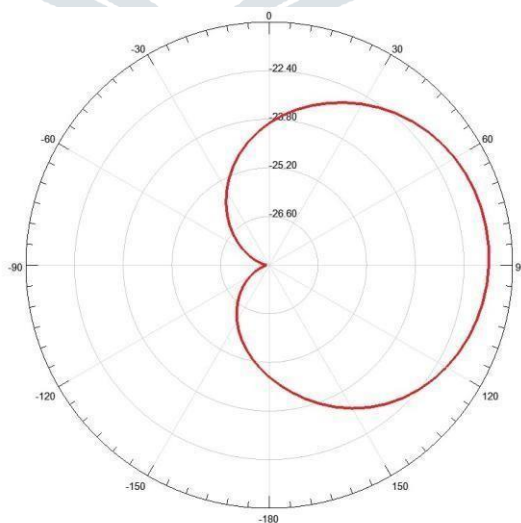


Fig.19 Y plane radiation pattern at 3.4GHz

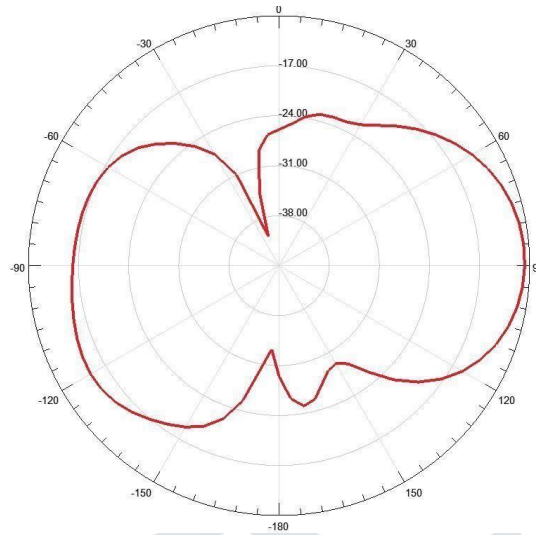


Fig.20 Y plane radiation pattern at 10GHz

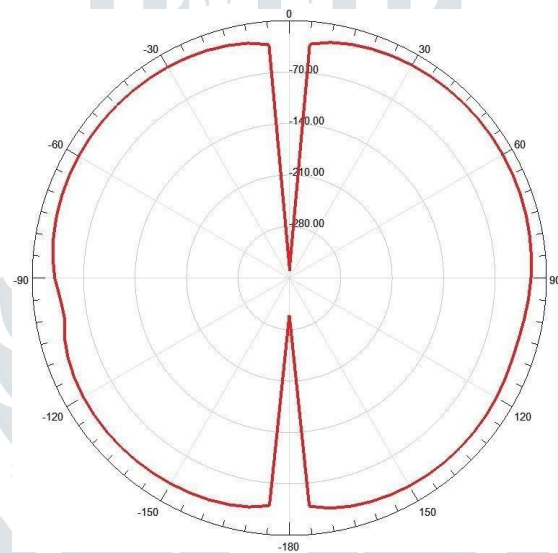


Fig.21 Z plane radiation pattern at 3.4GHz

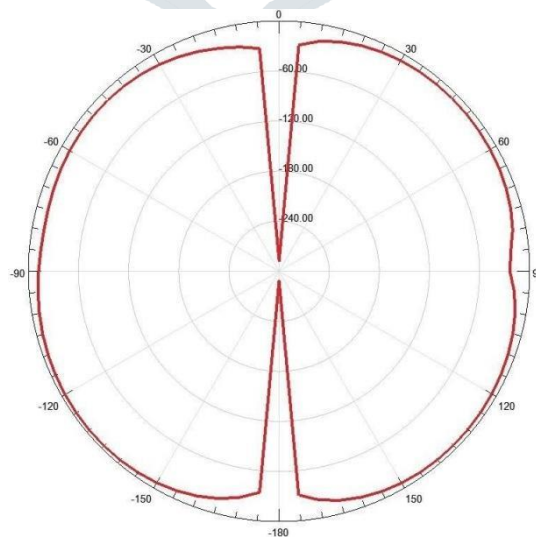


Fig.22 Z plane radiation pattern at 10GHz

## VII. PROPOSED ANTENNA IN WLAN APPLICATIONS

Fig.23 shows the Wi-Fi Router with Existing Antennas and the results are shown in Fig.24 with download speed of 10.9 mbps and upload speed of 13.0 mbps. We replaced the existed antennas with proposed antennas as shown in the Fig. 25, and the results are fine enough as compared to existed Wi-Fi Router with Download speed of 11.7Mbps and Upload speed of 12.3 Mbps as shown in the Fig.26.



Fig.23 Wi-Fi Router with Existing Antennas

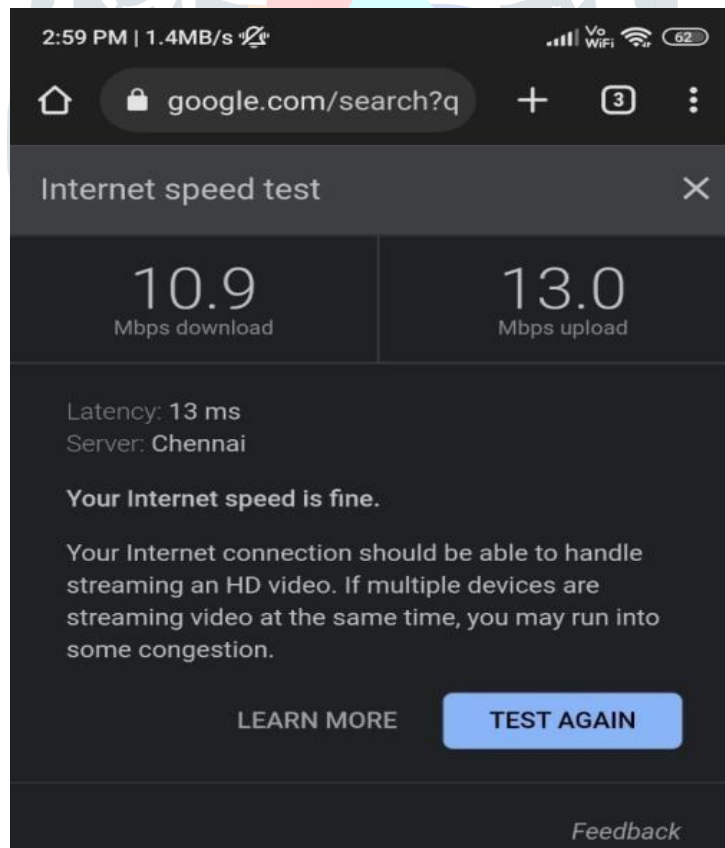


Fig.24 Results of Wi-Fi Router with Existing Antennas

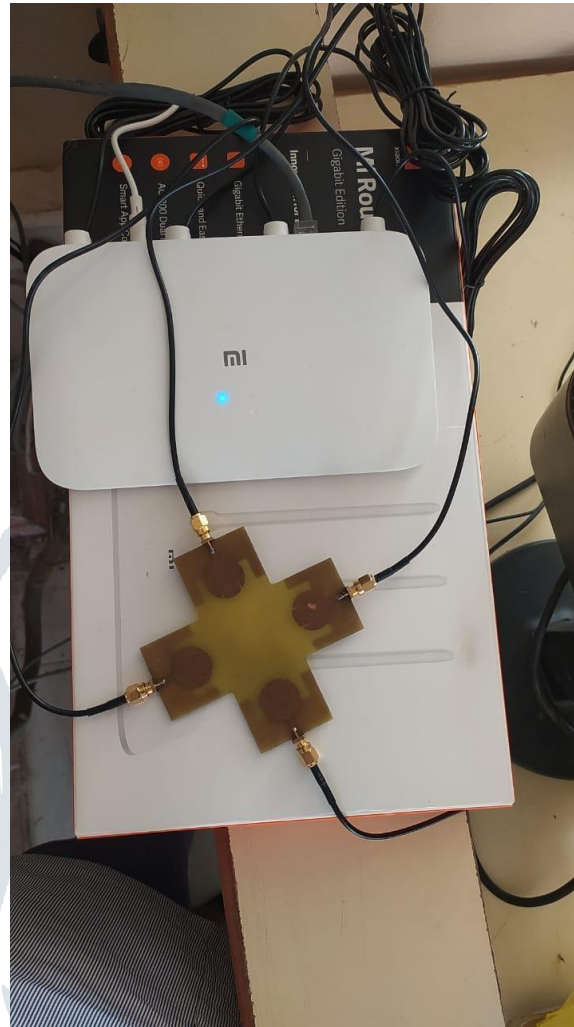


Fig.25 Wi-Fi Router with Proposed Antenna

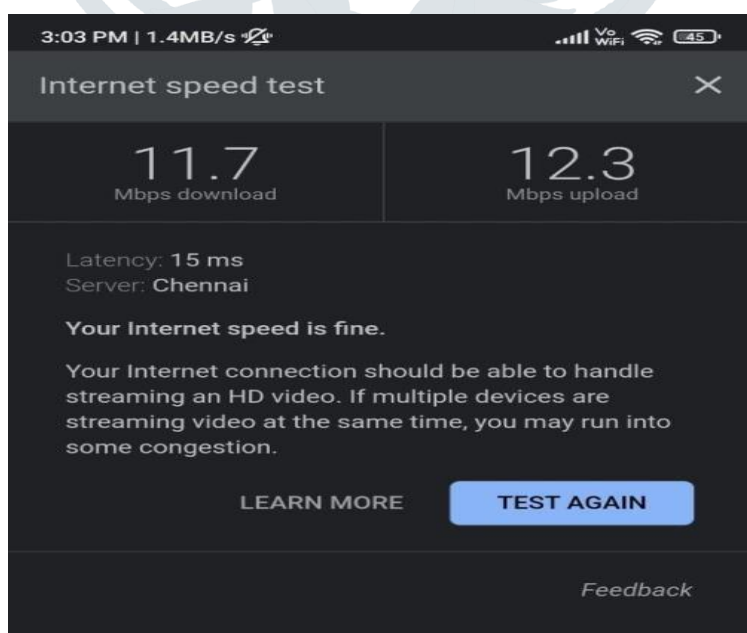


Fig.26 Results of Wi-Fi Router with Proposed Antenna

## VIII. CONCLUSION

For 5G systems, an orthogonal 4 element MIMO antenna (102\*102\*1.6mm<sup>3</sup>) with integrated ground structure of FR-4 is proposed. The work is based on design methods, performance-based performance parameters, augmented antenna design, and detailed MIMO diversity analysis. The circular patched is essential for achieving maximum bandwidth in construction. Antennas in the 2x2 MIMO provide about 85 percent bandwidth (24.8 GHz to 26.0 GHz), more over 20dB systematic separation, radiation patterns involving in all directions, Envelop Correlation Coefficient value is 0.08, DG =9.99 dB, medium gain is > 5.6dB and Efficiency is of 82.0 percent. This antenna is well-isolated, has a low ECC (0.08), and provides strong diversity. The suggested antenna achieves stable gain, directional radiation patterns, and impedance bandwidth with dual notches, which are proven by MIMO antenna research results. Adequate antenna performance for 5G MIMO applications and it is also applicable in WLAN applications (Wi-Fi Router).

## REFERENCES

- [1] T.S. Rappaport, S. Sun, R. Mayzus, H. Zhao, Y. Azar, K. Wang, G.N. Wong, J.K. Schulz, M. Samimi, F. Gutierrez, Millimeter wave mobile communications for 5G cellular: It will work, *IEEE Access* 1 (2013) 335–349.
- [2] R.G. Vaughan, J.B. Andersen, Antenna diversity in mobile communications, *IEEE Trans. Veh. Technol.* 36 (4) (1987) 149–172.
- [3] Z. Pi, F. Khan, An introduction to millimeter-wave mobile broadband systems, *IEEE Commun. Mag.* 49 (6) (2011) 101–107.
- [4] S. Kim, E. Visotsky, P. Moorut, K. Bechta, A. Ghosh, and C. Dietrich, “Coexistence of 5G with the incumbents in the 28 and 70 GHz bands,” *IEEE J. Sel. Areas Commun.*, vol. 35, no. 6, pp. 1254–1268, Jun. 2017.
- [5] J.-H. Lee, J.-S. Choi, and S.-C. Kim, “Cell coverage analysis of 28 GHz millimeter wave in urban microcell environment using 3-D ray tracing,” *IEEE Trans. Antennas Propag.*, vol. 66, no. 3, pp. 1479–1487, Mar. 2018.
- [6] A. Desai, T. Upadhyaya, R. Patel, Compact wideband transparent antenna for 5G communication systems, *Microw Opt Technol Lett* 61 (3) (2019) 781–786.
- [7] R. Krishnamoorthy, A. Desai, R. Patel, A. Grover, 4 Element compact triple band MIMO antenna for sub-6 GHz 5G wireless applications, *Wireless Netw.* (2021) 1–13.
- [8] M.S. Sharawi, Current misuses and future prospects for printed multiple-input, multiple-output antenna systems [wireless corner], *IEEE Antennas Propag. Mag.* 59 (2) (2017) 162–170.
- [9] Irshad Khan, Muhammad, Muhammad Irfan Khattak, Saeed Ur Rahman, Abdul Baseer Qazi, Ahmad Abdeltawab Telba, and Abdelrazik Sebak. “Design and investigation of modern UWB-MIMO antenna with optimized isolation.” *Micromachines* 11, no. 4 (2020): 432.
- [10] J. Banerjee, A. Karmakar, R. Ghatak, D.R. Poddar, Compact CPW-fed UWB MIMO antenna with a novel modified Minkowski fractal defected ground structure (DGS) for high isolation and triple band-notch characteristic, *Journal of electromagnetic Waves and Applications* 31 (15) (2017) 1550–1565.
- [11] I. Nadeem, D.-Y. Choi, Study on mutual coupling reduction technique for MIMO antennas, *IEEE Access* 7 (2019) 563–586.
- [12] N. Kumar, K. Usha Kiran, Meander-line electromagnetic bandgap structure for UWB MIMO antenna mutual coupling reduction in E-plane, *AEU- International Journal of Electronics and Communications* 127 (2020) 153423, <https://doi.org/10.1016/j.aeue.2020.153423>.
- [13] A. Ramachandran, S. Mathew, V. Rajan, V. Kesavath, A compact triband quad-element MIMO antenna using SRR ring for high isolation, *IEEE Antennas Wirel. Propag. Lett.* 16 (2017)1409–1412.
- [14] M. Sonkki, D. Pfeil, V. Hovinen, K.R. Dandekar, Wideband Planar Four-Element Linear Antenna Array, *IEEE Antennas Wirel. Propag. Lett.* 13 (2014) 1663–1666.
- [15] A. MoradiKordalivand, T.A. Rahman, M. Khalily, Common Elements Wideband MIMO Antenna System for WiFi/LTE AccessPoint Applications, *IEEE Antennas Wirel. Propag. Lett.*13 (2014) 1601–1604.
- [16] H. Wang, L. Liu, Z. Zhang, Y. Li, Z. Feng, A Wideband Compact WLAN/WiMAX MIMO Antenna Based on Dipole With V-shaped Ground Branch, *IEEE Trans. Antennas Propag.* 63 (5) (2015) 2290–2295.
- [17] R. Anitha, P.V. Vinesh, K.C. Prakash, P. Mohanan, K. Vasudevan, A Compact Quad Element Slotted Ground Wideband Antenna for MIMO Applications, *IEEE Trans. Antennas Propag.* 64 (10) (2016) 4550–4553.
- [18] A. Desai, M. Palandoken, J. Kulkarni, G. Byun, T.K. Nguyen, “Wideband Flexible/Transparent Connected-Ground MIMO Antennas for Sub-6 GHz 5G and WLAN Applications,” in *IEEE, Acces* 9 (2021) 147003–147015, <https://doi.org/10.1109/ACCESS.2021.3123366>.
- [19] M. Usman, E. Kobal, J. Nasir, Y. Zhu, C. Yu, A. Zhu, Compact SIW Fed Dual-Port Single Element Annular Slot MIMO Antenna for 5G mmWave Applications, *IEEE Access* 9 (2021) 91995–92002.

- [20] W. Ali, S. Das, H. Medkour, S. Lakrit, Planar dual- band 27/39 GHz millimeter-wave MIMO antenna for 5G applications, *Microsyst Technol* 27 (1) (2021) 283–292, <https://doi.org/10.1007/s00542-020-04951-1>.
- [21] Z. Wani, M.P. Abegaonkar, S.K. Koul, A 28- GHz antenna for 5G MIMO applications, *Progress In Electromagnetics Research Letters* 78 (2018) 73–79.
- [22] M.M. Kamal, S. Yang, X.-C. Ren, A. Altaf, S.H. Kiani, M.R. Anjum, A. Iqbal, M. Asif, S.I. Saeed, Infinity Shell Shaped MIMO Antenna Array for mm-Wave 5G Applications, *Electronics* 10 (2) (2021) 165, <https://doi.org/10.3390/electronics10020165>.
- [23] Raheel, Kiran, Ahsan Altaf, Arbab Waheed, Saad Hassan Kiani, Daniyal Ali Sehrai, Faisal Tubbal, and Raad Raad. “E-shaped H-slotted dual band mmwave antenna for 5G technology.” *Electronics* 10, no. 9 (2021): 1019.
- [24] A. Desai, C.D. Bui, J. Patel, T. Upadhyaya, G. Byun, T.K.Nguyen, Compact Wideband Four Element Optically Transparent MIMO Antenna for mm- Wave 5G Applications, *IEEE Access* 8 (2020) 194206–194217.
- [25] Khalid, Mahnoor, Syeda Iffat Naqvi, Niamat Hussain, MuhibUr Rahman, Seyed Sajad Mirjavadi, Muhammad Jamil Khan, and Yasar Amin. “4-Port MIMO antenna with defected ground structure for 5G millimeter wave applications.” *Electronics* 9, no. 1 (2020): 71.
- [26] Rahman, Saifur, Xin-cheng Ren, Ahsan Altaf, Muhammad Irfan, Mujeeb Abdullah, Fazal Muhammad, Muhammad Rizwan Anjum, Salim Nasar Faraj Mursal, and Fahad Salem AlKahtani. “Nature inspired MIMO antenna system for futuremmWave technologies.” *Micromachines* 11, no. 12(2020): 1083.
- [27] Jilani, S.F. and Alomainy, A., 2018. Millimeter- wave T-shapedMIMO antenna with defected ground structures for 5G cellular networks. *IET Microwaves, Antennas & Propagation*, 12(5), pp.672-677. IET
- [28] D. Pozar, *Surface wave effects for millimetre wave printed antennas* vol. 21 (1983) 692–695.
- [29] N.A. Touhami, T. Elhamadi, M.A. Ennasar, High-gain and broadband SIW cavity-backed slots antenna for X-band applications, *Int. J. Microwave Wireless Technol.* (2021) 1–8.
- [30] S.A. Saputro, S. Nandiwardhana, J.-Y. Chung, Estimation of Antenna Correlation Coefficient of N-Port Lossy MIMO Array, *ETRI Journal* 40 (3) (2018) 303–308.

